THE ASTROPHYSICAL JOURNAL, 563:361–366, 2001 December 10

X-RAY DETECTION FROM BONA FIDE AND CANDIDATE BROWN DWARFS IN THE ρ OPHIUCHI CLOUD WITH *CHANDRA*

KENSUKE IMANISHI, MASAHIRO TSUJIMOTO, AND KATSUJI KOYAMA
Department of Physics, Graduate School of Science, Kyoto University, Sakyo-ku, Kyoto 606-8502, Japan; kensuke@cr.scphys.kyoto-u.ac.jp, tsujimot@cr.scphys.kyoto-u.ac.jp, koyama@cr.scphys.kyoto-u.ac.jp
Received 2001 June 24; accepted 2001 August 7

ABSTRACT

We present results of an X-ray search from bona fide and candidate brown dwarfs in the ρ Ophiuchi cloud cores with the *Chandra X-ray Observatory*. The selected areas are two fields near the cloud center and are observed with the ACIS-I array of a $17' \times 17'$ size and a $\sim$100 ks exposure. Among 18 bona fide and candidate brown dwarfs listed by the infrared spectroscopy, we find X-ray emission from seven sources above 99.9% confidence level. Therefore, $\sim$40% of the infrared-selected brown dwarfs in this cloud emit X-rays. For the brightest four sources, the X-ray spectra are made and are fitted with a thin-thermal plasma model of a temperature 1–2.5 keV. The X-rays are also time variable with rapid flares from two of the brown dwarfs. Assuming 2 keV temperature and using the empirical relation of A_V versus N_H, we estimate the X-ray luminosity or its upper limit of the other faint or non–X-ray sources. The X-ray luminosity (L_X) of the X-ray-detected sources is in the range of 0.3–90 $\times 10^{28}$ ergs s^{-1}, while the luminosity ratio of X-ray to bolometric (L_X/L_{bol}) is 10^{-5}–10^{-3}, similar to those of low-mass pre–main-sequence and dMe stars. All these results suggest that the X-ray origin of brown dwarfs is the same as low-mass stars; strong magnetic activity at the stellar surface.

Subject headings: ISM: individual (ρ Ophiuchi Cloud) — stars: low-mass, brown dwarfs — X-rays: stars

1. INTRODUCTION

Brown dwarfs are substellar objects with mass well below the hydrogen burning limit ($\sim$0.08 $M_\odot$), which fill up the gap between stars and planets. With no stable nuclear burning, the energy source of brown dwarfs is gravitational contraction, hence brown dwarfs become cooler and less luminous with the increasing ages. *ROSAT* detected X-rays from several brown dwarfs and their candidates in star-forming regions; Chamaeleon, ρ Ophiuchi (ρ Oph), and Taurus (Neuhäuser & Comrerón 1998; Neuhäuser et al. 1999). X-ray flares from field brown dwarfs were also found (Fleming, Giampapa, & Schmitt 2000; Rutledge et al. 2000). These X-ray features are similar to those of low-mass stars, hence the X-rays are likely to be magnetic origin. However, the standard (α-ω) dynamo to produce the magnetic activity may not be present, because brown dwarfs are fully convective, hence there are no anchor points of the magnetic field in the star interior (Drake et al. 1996). In order to address the X-ray features and to study the emission mechanisms of brown dwarfs, our current knowledge is still very poor, due mainly to the limited sensitivity of the previous instruments. This observational constrain is largely relaxed by the *Chandra X-ray Observatory* of wide band sensitivity (0.5–10.0 keV) coupled with unprecedented spatial resolution of $\sim$0.″5 (Weisskopf, O'dell, & van Speybroeck 1996). We systematically search and study X-rays from brown dwarfs in one of the nearest star-forming regions, using the data of two deep ACIS-I exposures on the ρ Oph molecular cloud cores.

2. OBSERVATIONS AND DATA REDUCTION

Two *Chandra* observations were made on the central region of the ρ Oph cloud with the ACIS-I array consisting of four abutted X-ray CCDs. The first observation (here and after, obs. 1) covered a $17.'4 \times 17.'4$ area including cores B, C, E, and F, while the second observation (obs. 2) covered the center of core A (Motte, André, & Neri 1998). The level 2 data are retrieved from the *Chandra* X-ray Center (CXC) archive, in which the data degradation caused by the increase of charge transfer inefficiency (CTI) in orbit is corrected. X-ray events are selected with the *ASCA* grades 0, 2, 3, 4, and 6. After the processing, $\approx$100 ks effective exposure time is obtained from each observation. The log of the observations is listed in Table 1.

In these two fields, 18 late M dwarfs have been reported, based on the water vapor absorption at $\lambda = 2.4$–2.5 μm (Wilking, Greene, & Meyer 1999; Cushing, Tokunaga, & Kobayashi 2000). Among them, eight sources have the upper limit of mass less than 0.08 $M_\odot$, which we call "bona fide brown dwarfs" (here and after, BDs). The other 10 sources have a mass in the transition region of 0.08 $M_\odot$, hence called "candidate brown dwarfs" (CBDs). Their names and spectral types are shown in Table 2.

3. ANALYSIS AND RESULTS

3.1. *Source Detection*

Using the "wavdetect"[1] command, we pick up $\sim$100 X-ray sources from each field above the significance criterion of 10^{-7}. Infrared (IR) counterparts from the catalog of Barsony et al. (1997) are searched and the position is cross-correlated to that of the X-ray source. Systematic coordinate offset of the *Chandra* frame is then fine-tuned to fit the IR frame. After the offset correction, the relative position error (1 σ) is 1.″2. We find X-ray counterparts from five IR positions in a 2 σ error radius (2.″4) out of the 18 cataloged BDs and CBDs (GY 310, GY 31, GY 37, GY 59, and GY 326). The X-ray positions and relative offsets from the IR sources are given in Table 2. The X-ray counts are extracted from a circle of a half-radius of the point-spread function (PSF) around the X-ray position.

Since no apparent X-ray sources are found in a 2 σ error radius (2.″4) of the other 13 cataloged BDs and CBDs, we

[1] See http://asc.harvard.edu/udocs/docs/swdocs/detect/html/.

TABLE 1

LOG OF THE *Chandra* ACIS-I OBSERVATIONS ON THE ρ OPHIUCHI CLOUD CORES

Obs.ID	Sequence ID	Date	R.A.[a] (J2000)	Decl.[a] (J2000)	Exposure (ks)
1.....	200060	2000 Apr 13–14	16 27 18.1	−24 34 21.9	100.6
2.....	200062	2000 May 15–17	16 26 35.3	−24 23 12.9	96.4

[a] The position of the telescope optical axis. Units of right ascension are hours, minutes, and seconds, and units of declination are degrees, arcminutes, and arcseconds.

define a circle with a half-radius of PSF around each IR position. Then we manually count the X-ray photons in the circle. We note that a rather small source radius is selected so as to maximize the signal-to-noise (S/N) ratio, particularly, for faint X-ray sources. Nevertheless, as is demonstrated in the 5 bright sources, the position error between IR and X-rays is always smaller than the source radius, because both have generally similar dependence on the source off-axis angle; both have the smaller values for the sources with smaller off-axis angle. Therefore, most of the X-ray photons for the relevant BDs and CBDs, if any, may fall in the source circles. The X-ray flux thus counted are given in Table 2.

The mean background counts are estimated from source-free regions of a 63 arcmin^2 and a 59 arcmin^2 area in the ACIS-I fields for obs. 1 and obs. 2, respectively. The soft band (0.5–2.0 keV) background counts (in units of 10^{-2} counts arcsec^{-2}) are 2.3 and 2.2, for obs. 1 and obs. 2, respectively, while those in the hard (2.0–9.0 keV) band are about 3 times larger, 6.8 and 6.5 for obs. 1 and obs. 2. The background counts in each source area are given in Table 2. We then separately calculate the confidence level (CL) of the X-ray detection for the soft, hard, and total (0.5–9.0 keV) bands. Based on the Poisson statistics, the CL is defined as;

$$CL = \sum_{N'=0}^{N_0-1} e^{-N_{\rm bg}} \frac{N_{\rm bg}^{N'}}{N'!},$$

where N_0 and $N_{\rm bg}$ are the detected and the background counts in the source circle, respectively (see e.g., Gehrels 1986, and references therein). We set the detection (or the upper limit) criterion that the CL should be larger than

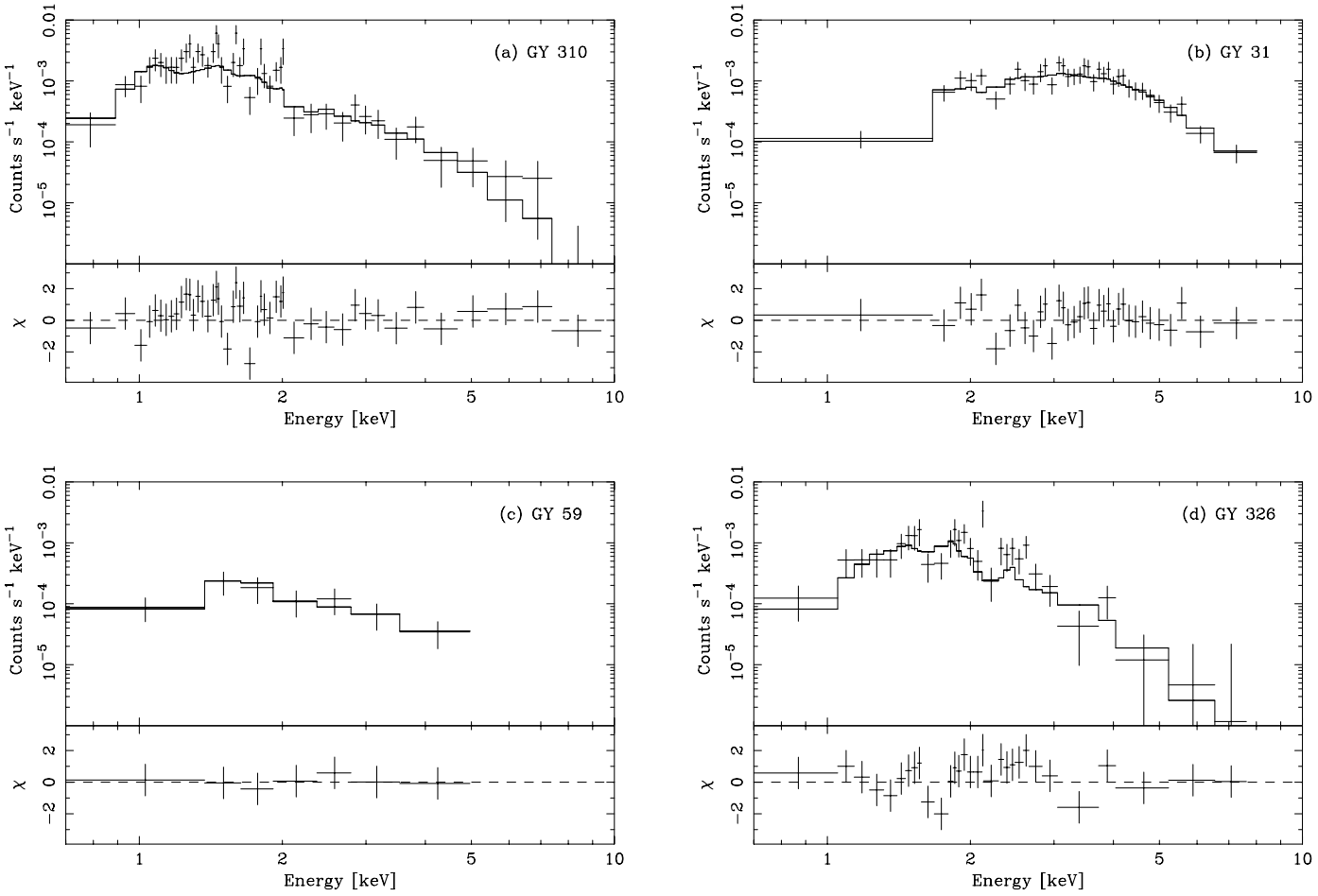

FIG. 1.—Spectra of (*a*) GY 310, (*b*) GY 31, (*c*) GY 59, and (*d*) GY 326. The upper panels show data points (*crosses*) and the best-fit model (*solid line*), while the lower panels are the data residuals from the best-fit model.

TABLE 2

BONA FIDE AND CANDIDATE BROWN DWARFS IN THE ρ OPHIUCHI CLOUD CORES

NAME	SPECTRAL TYPE[a]	ID[b]	R. A.[c] (J2000)	DECL.[c] (J2000)	OFFSET[d] (arcsec)	PSF[e] (arcsec)	X-RAY COUNTS[f] Soft	Hard	BGD	$1-CL$[g]	L_X[h] (10^{28}ergs s^{-1})	log (L_X/L_{bol})	REFERENCE
Brown Dwarf (BD)													
CRBR 14...	M7.5	2	...	...	...	5.7	3	2	0.5	ND (S)	<0.55	<−4.3	1
GY 10	M8.5	2	...	...	...	3.2	2	0	0.2	ND (S)	<0.48	<−4.5	1
GY 11	M6.5	2	...	...	...	3.3	1	1	0.2	ND (T)	<0.12	<−3.8	1, 2
CRBR 31...	M6.7	2	...	...	...	7.1	0	2	0.9	ND (H)	<0.56	<−3.6	2
GY 64	M8	2	...	...	...	3.7	1	0	0.2	ND (S)	<0.93	<−3.5	1, 2
GY 141.....	M8	1	...	...	...	9.0	7	1	1.5	8.0×10^{-4} (S)	0.25	−3.6	2
		2	...	...	...	22.3	11	23	8.6	ND (S)	<0.33	<−3.5	
GY 202.....	M7	1	...	...	...	9.4	2	4	1.6	ND (S)	<1.2	<−3.7	1
		2	...	...	...	16.8	3	9	4.9	ND (S)	<2.0	<−3.4	
GY 310.....	M8.5	1	$27^m38^s.6$	38′39″.1	1.3	9.2	182	59	1.5	$<1.0 \times 10^{-15}$ (T)	9.3	−3.4	1
Candidate Brown Dwarf (CBD)													
CRBR 15...	M5	2	...	...	...	4.2	2	1	0.3	ND (S)	<1.1	<−4.2	1
GY 5	M7	2	...	...	...	4.7	2	1	0.4	ND (S)	<0.16	<−5.2	1
GY 31	M5.5	2	$26^m25^s.2$	23′25″.7	0.2	2.5	41	350	0.1	$<1.0 \times 10^{-15}$ (T)	93	−3.5	1
GY 37	M6	2	$26^m27^s.8$	26′43″.9	0.8	4.2	7	5	0.3	3.7×10^{-8} (S)	0.59	−4.2	1
GY 59	M6	2	$26^m31^s.4$	25′32″.2	0.7	2.6	17	22	0.1	$<1.0 \times 10^{-15}$ (T)	2.6	−3.9	1
GY 84	M6	2	...	...	...	1.9	2	2	0.1	1.3×10^{-4} (T)	0.85	−4.7	1
GY 163.....	M2.5	1	...	...	...	12.4	5	12	2.8	ND (T)	<12	<−3.8	1
		2	...	...	...	11.9	3	7	2.4	ND (S)	<10	<−3.8	
GY 218.....	M4.0	1	...	...	...	7.2	2	3	0.9	ND (S)	<0.45	<−3.6	2
CRBR 67...	M4.4	1	...	...	...	3.2	0	0	0.2	ND (–)	<0.31	<−3.5	2
GY 326.....	M4	1	$27^m42^s.8$	38′51″.1	1.5	11.4	67	65	2.3	$<1.0 \times 10^{-15}$ (T)	28	−3.4	1

[a] Spectral type determined from the water vapor absorption.

[b] Observation identification (see Table 1).

[c] Position of the identified X-ray source which is picked up with the "wavdetect" command (see § 3.1). Right ascension and declination for all sources are at 16^h and $-24°$. Units of right ascension are minutes and seconds, and units of declination are arcminutes and arcseconds.

[d] Offset between the IR and the X-ray sources.

[e] Radius of the point-spread function.

[f] X-ray counts in the soft (0.5–2.0 keV) and hard (2.0–9.0 keV) bands, and predicted background counts in the soft band within the source circle. Background counts in the hard band is $\sim$3 times larger than those in the soft band.

[g] CL is the confidence level of the source detection (see § 3.1). Parentheses indicate the energy band in which the maximum CL-value is obtained (S: 0.5–2.0 keV, H: 2.0–9.0 keV, T: 0.5–9.0 keV). ND represents non–X-ray detection with $CL < 0.999$ (i.e., $1 - CL > 10^{-3}$).

[h] Absorption-corrected luminosity in 0.5–9.0 keV. The distance to each source is assumed to be 145 pc (de Zeeuw et al. 1999).

REFERENCES.—(1) Wilking et al. 1999; (2) Cushing et al. 2000.

TABLE 3

BEST-FIT PARAMETERS OF THE BRIGHTEST FOUR SOURCES

Name	kT[a] (keV)	log (EM)[a] (cm^{-3})	N_H[a] ($10^{22} cm^{-2}$)	χ^2/d.o.f.
GY 310.....	1.7(0.9–2.2)	51.6(51.5–52.1)	0.8(0.5–1.5)	57.8/44
GY 31	2.2(1.7–2.9)	52.6(52.4–52.8)	5.9(5.1–7.2)	25.1/33
GY 59	2.5(>1.0)	51.0(50.6–51.7)	1.4(0.5–3.0)	0.556/4
GY 326.....	0.9(0.7–1.2)	52.1(51.7–52.4)	2.3(1.6–3.0)	34.8/28

[a] Parentheses indicate the 90% confidence limits.

0.999 ($=3.3\ \sigma$) in any of the three energy band data. In Table 2, we show the maximum CL-value for each source. For sources located in both fields of view (GY 141, GY 163, and GY 202), we also estimate the CL for the combined data as well as the separate data. However, no higher CL-value is obtained from all the sources.

As are summarized in Table 2, bright X-rays are found from three CBDs (GY 31, GY 37, and GY 59) in addition to previously reported sources, GY 310 and GY 326 (Imanishi, Koyama, & Tsuboi 2001). Detection of X-rays from a CBD, GY 84 is also highly significant. Another BD, GY 141 in obs. 1, show faint X-rays with CL of ≥ 0.999 in the soft band. Using the log$N$–log$S$ relation by Mushotzky et al. (2000), we estimate the chance coincidence of a background source to fall in the source circle to be 0.6%–1%, where the uncertainty mainly comes from the ambiguity of the amount of interstellar absorption. Furthermore, background sources are most likely AGNs and may have harder spectra than the possible counterpart of GY 141. We thus conclude that the faint X-rays from this BD are real.

3.2. *X-Ray Spectra and Luminosities*

For the brightest four sources—one BD (GY 310) and three CBDs (GY 31, GY 59, and GY 326)—we analyze the time-averaged X-ray spectra. The background spectra are extracted from the same regions used in § 3.1. We then fit the spectra with a thin-thermal plasma (MEKAL: Mewe, Gronenschild, & van den Oord 1985) model, in which the

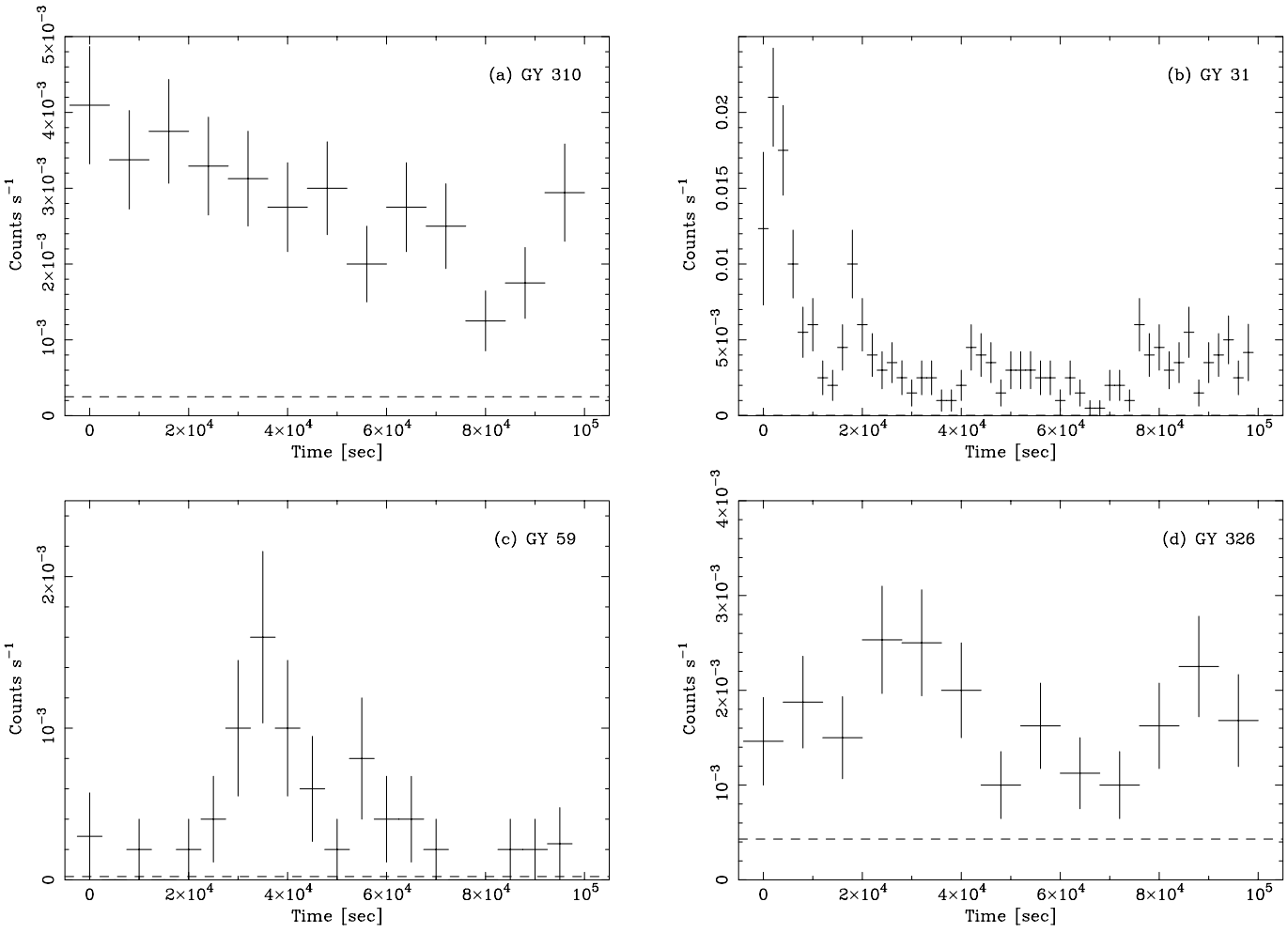

FIG. 2.—Light curves of (*a*) GY 310, (*b*) GY 31, (*c*) GY 59, and (*d*) GY 326 in the 0.5–9.0 keV band. The background level is shown by the dashed line. For GY 31, the background line ($\sim 2 \times 10^{-5}$ counts s^{-1}) overlaps with the bottom solid line.

metal abundance is fixed to 0.3 solar based on the fitting results of other *Chandra* X-ray sources in this region (Imanishi et al. 2001). The spectra and the best-fit parameters are shown in Figure 1 and Table 3. The best-fit plasma temperature (kT) is in the range of 0.9–2.5 keV. Small differences in the parameters of GY 310 and GY 326 from those in Table 1 of Imanishi et al. (2001), which is nevertheless unimportant, would be attributed to the more elaborated data-reduction process of this paper (see § 2 in Imanishi et al. 2001).

For the faint or non–X-ray sources, the spectrum is assumed to be a thin-thermal plasma of 2 keV temperature (the mean value for the bright sources), while the absorption column is estimated from the empirical relation, $N_{\rm H} = 1.59 \times 10^{21}\ A_V\ {\rm cm}^{-2}$ (Imanishi et al. 2001), where A_V is the visual extinction derived from IR photometry (Wilking et al. 1999; Cushing et al. 2000). We then calculate the X-ray luminosities or those of the 99.9% upper limits in the soft band (Table 2).

3.3. *Time Variability*

Figure 2 shows the light curves of (*a*) GY 310, (*b*) GY 31, (*c*) GY 59, and (*d*) GY 326 in 0.5–9.0 keV, where the background levels are represented by the dashed lines. For GY 31 and GY 59, clear flarelike events, typical to those of low-mass main-sequence and pre–main-sequence stars, a fast rise and slow decay, are seen. The flare-decay timescale ($\sim 10^4$ s) is also the same as that of low-mass stars.

GY 310 and GY 326, on the other hand, show no clear flare, but exhibit aperiodic variability of flux change by a factor of ~ 2 within 100 ks exposure. Since we see no large intensity variation in the background flux, we conclude that the variability is highly significant.

In order to search for spectral change during the flare, we separately make and fit the spectra of GY 31 in the flare and quiescent phases. A hint of spectral hardening during the flare is found, although it is not significant from the statistical point of view; kT is $2.5^{+0.9}_{-0.7}$ keV at the first flare then decreases to $2.1^{+0.6}_{-0.5}$ keV in a rather quiescent phases.

4. DISCUSSION

We detect X-ray emission from two out of eight BDs and five out of 10 CBDs in the ρ Oph cloud cores. The X-ray detection rate is thus 25% (BD) and 50% (CBD). Neuhäuser et al. (1999) claimed the X-ray detection of only one BD (GY 202) with *ROSAT*/PSPC, in the same fields of the present observations. Our present observations find no X-ray from GY 202 with an upper limit of 1.2×10^{28} ergs s^{-1}. Instead, we find a class I candidate WL 1 (No.13, in Imanishi et al. 2001) within the PSPC error circle of GY 202. This source emits X-rays with comparable luminosity to that of GY 202 reported with *ROSAT*/PSPC. Conversely, Neuhäuser et al. (1999) found no X-ray with an upper limit of $\sim 10^{28}$ ergs s^{-1} from all the *Chandra* detected sources. They, however, estimated the X-ray luminosity assuming $kT = 1$ keV and $A_v =$ few mag (i.e., $N_{\rm H} =$ few $\times 10^{21}$ cm^{-2}), which may be significantly lower than the real case (see Table 3). We hence reestimate the upper limit with the same assumption adopted in this paper (§ 3.2), then find that the *ROSAT* upper limit could be nearly 1 or 2 orders of magnitude higher than those of the original paper. If we adopt these newly estimated upper limits, we find no significant flux change from the *ROSAT* to the *Chandra* era.

In Table 2, we display the ratio of the X-ray ($L_{\rm X}$) and bolometric ($L_{\rm bol}$) luminosities. $L_{\rm bol}$ is roughly proportional to the area of the photosphere, hence $L_{\rm X}/L_{\rm bol}$ is a good indicator of coronal X-ray activity per unit surface area. The $L_{\rm X}/L_{\rm bol}$-value lies between 10^{-5} and 10^{-3}, which is similar to low-mass pre–main-sequence stars (e.g., Imanishi et al. 2001) and dMe stars (Giampapa et al. 1996) but is significantly higher than that of the quiescent solar corona: $\sim 5 \times 10^{-7}$ (Vaiana & Rosner 1978). It should also be noted that most of the upper limits of $L_{\rm X}/L_{\rm bol}$ of X-ray nondetected BDs and CBDs are scattered around 10^{-5}–10^{-3}, which are comparable with or slightly lower than those of X-ray detected BDs and CBDs. This leads us to suspect that these X-ray nondetected BDs and CBDs may emit X-rays below but near at the current sensitivity limit of *Chandra*.

We also obtain the X-ray spectra from one BD and three CBDs for the first time (§ 3.2), which are fitted with a thin thermal plasma model of ~ 2 keV temperature. Solar-like flares are also detected from two CBDs (GY 31 and GY 59, § 3.3). These X-ray features are similar to those of low-mass stars. Together with the high $L_{\rm X}/L_{\rm bol}$-value, we suggest that X-rays from BDs and CBDs are attributable to magnetic activities like low-mass stars. Detection of highly variable radio emission from GY 31, which probably arises from nonthermal gyrosynchrotron emission, also indicates the existence of strong and time variable magnetic activity (P. André 1999, private communication; see Neuhäuser et al. 1999).

One debatable issue is the mechanism of magnetic field amplification. Brown dwarfs are fully convective, hence the standard dynamo (α-ω dynamo) mechanism may not work. This situation is the same as low-mass protostars. As one possible scenario, Montmerle et al. (2000) proposed an amplification of the magnetic field between the star and the circumstellar disk by twisting through the differential rotation. If BDs and CBDs emit X-rays with the same mechanism, X-ray activity should vanish when the circumstellar disk disappears as the star evolves. Figure 3 shows the relation between the excess emission at K-band and the

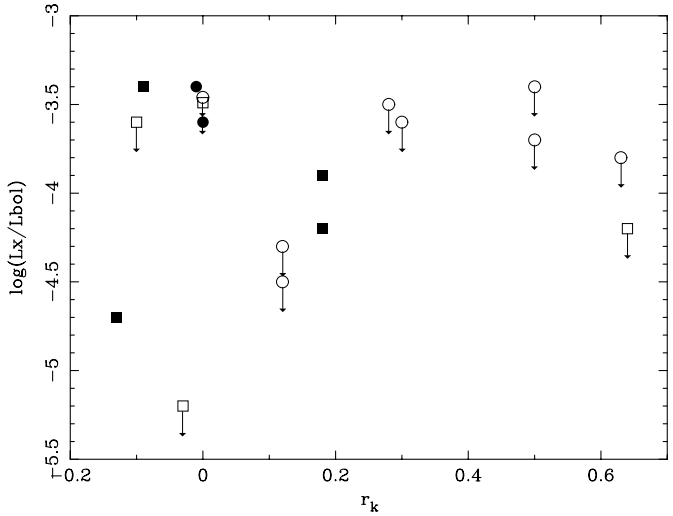

FIG. 3.—Plots of the excess emission at K-band (r_k) and the luminosity ratio between X-ray and bolometric ($L_{\rm X}/L_{\rm bol}$). Circles and squares represent BDs and CBDs, respectively. X-ray detection and nondetection are indicated by filled and open symbols, respectively. Arrows indicate the upper limits. GY 31 and GY 163 are not included in this figure because no r_k-value has been obtained.

L_X/L_{bol}-value. The excess emission is defined as $r_k = F_{K_{ex}}/F_K$, where $F_{K_{ex}}$ is the flux from excess (circumstellar) emission and F_K is the stellar flux at K-band (Wilking et al. 1999; Cushing et al. 2000), hence $r_k > 0$ indicates the presence of the circumstellar disk. X-ray detected BDs and CBDs are uniformly distributed over two regions of $r_k > 0$ and $r_k \leq 0$; we see no hint that X-ray activity decreases as the circumstellar disk disappears ($r_k \leq 0$). We therefore conclude that the existence of the disk is not the key parameter in X-ray emission of BDs and CBDs. Another type of dynamo, such as turbulent-driven (α^2) dynamo (Durney, De Young, & Roxburgh 1993), is conceivable.

The authors express their thanks to Thomas Preibisch for critical refereeing and useful comments. The authors also acknowledge Yohko Tsuboi and Jun Yokogawa for useful discussions and comments. K. I. and M. T. are financially supported by JSPS Research Fellowship for Young Scientists.

REFERENCES

Barsony, M., Kenyon, S. J., Lada, E. A., & Teuben, P. J. 1997, ApJS, 112, 109
Cushing, M. C., Tokunaga, A. T., & Kobayashi, N. 2000, AJ, 119, 3019
de Zeeuw, P. T., Hoogerwerf, R., de Bruijne, J. H. J., Brown, A. G. A., & Blaauw, A. 1999, AJ, 117, 354
Drake, J. J., et al. 1996, ApJ, 469, 828
Durney, B. R., De Young, D. S., & Roxburgh, I. W. 1993, Sol. Phys., 145, 207
Fleming, T. A., Giampapa, M. S., & Schmitt, J. H. M. M. 2000, ApJ, 533, 372
Gehrels, N. 1986, ApJ, 303, 336
Giampapa, M. S., Rosner, R., Kashyap, V., Fleming, T. A., Schmitt, J. H. M. M., & Bookbinder, J. A. 1996, ApJ, 463, 707
Imanishi, K., Koyama, K., & Tsuboi, Y. 2001, ApJ, 557, 747
Mewe, R., Gronenschild, E. H. B. M., & van den Oord, G. H. J. 1985, A&AS, 62, 197
Montmerle, T., Grosso, N., Tsuboi, Y., & Koyama, K. 2000, ApJ, 532, 1097
Motte, F., André, P., & Neri, R. 1998, A&A, 336, 150
Mushotzky, R. F., Cowie, L. L., Barger, A. J., & Arnaud, K. A. 2000, Nature, 404, 459
Neuhäuser, R., & Comerón, F. 1998, Nature, 282, 83
Neuhäuser, R., et al. 1999, A&A, 343, 883
Rutledge, R. E., Basri, G., Martin, E. L., & Bildsten, L. 2000, ApJ, 538, L141
Vaiana, G. S., & Rosner, R. 1978, ARA&A, 16, 393
Weisskopf, M. C., O'dell, S. L., & van Speybroeck, L. P. 1996, Proc. SPIE, 2805, 2
Wilking, B. A., Greene, T. P., & Meyer, M. R. 1999, AJ, 117, 469

The Astrophysical Journal, 579:921, 2002 November 10

ERRATUM: "X-RAY DETECTION FROM BONA FIDE AND CANDIDATE BROWN DWARFS IN THE ρ OPHIUCHI CLOUD WITH *CHANDRA*" (ApJ, 563, 361 [2001])

Kensuke Imanishi, Masahiro Tsujimoto, and Katsuji Koyama
Department of Physics, Graduate School of Science, Kyoto University

Errors were made in the calculations of emission measures (EMs) using the best-fit normalizations in XSPEC. All the EMs in Table 3 should be multiplied by π; the log (EM) in the first row, for example, is 52.1(52.0–52.6), not 51.6(51.5–52.1). All the spectral parameters except EM are unchanged. These errors of EM do not affect any of the conclusions of the paper.